

Phases of Bosons or Fermions in confined optical lattices

H. Heiselberg

Univ. of S. Denmark, Campusvej 55, DK-5230 Odense M, Denmark

Phases of Bose or Fermi atoms in optical lattices confined in harmonic traps are studied within the Thomas-Fermi approximation. Critical radii and particle number for onset of Mott insulator states are calculated and phase diagrams shown in 1D, and estimated for 2 and 3D. Methods to observe these and novel phases such as d-wave superconductivity is discussed. Specifically the collective modes are calculated.

PACS numbers: 03.75.Ss, 71.10.Pm, 03.75.Lm

Cold quantum systems in optical lattice have been realized with Bose and Fermi atoms, and superfluid transitions to Mott insulator (MI) solids at filling $n = 1, 2, 3$ observed for bosons [1–4]. Luttinger and Luther-Emery liquids and MI solids appear for 1D fermions whereas in 2D it is believed that d-wave superconductivity (dSC or High T_c) appear between metal and antiferromagnetic (AFM) phases [5,6]. Likewise quantum spin phases [7], supersolids [8], fractional quantum Hall phases [9,10], mixed [11] and other phases may be studied.

By tuning the barriers of the optical lattices and the interaction strengths near or far from Feshbach resonances, the Fermi [12]: $H = -t \sum_{\langle ij \rangle \sigma} \hat{a}_{i\sigma}^\dagger \hat{a}_{j,\sigma} + U \sum_i \hat{n}_{i\uparrow} \hat{n}_{i\downarrow}$, and Bose [13]: $H = -t \sum_{\langle ij \rangle \sigma} \hat{a}_{i\sigma}^\dagger \hat{a}_{j,\sigma} + U \sum_i \hat{n}_{i\uparrow} \hat{n}_{i\downarrow}$, Hubbard models can be realized with any interaction and hopping strengths in 1, 2 and 3 dimensions [14,15]. Here, $\hat{a}_{i\sigma}$ and \hat{b}_i are the usual Fermi and Bose creation operators, $\langle ij \rangle$ sums over nearest neighbours $j = i \pm 1$, t is the hopping parameter to nearest site and U is the on-site interaction energy. Both can be expressed in terms of the lattice potential and particle interactions such as the s-wave scattering length (see, e.g. [14,15]). The optical lattices are in experiments usually confined in a trap typically in the form of a harmonic potential $V_i = V_2 r_i^2$. Here, the lattice point $r_i = id$ is an integer times the lattice spacing d . The optical lattices are then clean systems with controlled disorder and a number of MI, superfluid and other phases appear as the densities increase towards the center of the trap [14–20].

It is the purpose here to calculate the phase diagram for these models in the Thomas-Fermi approximation (TF) at zero temperature, which can be done analytically for strong and weak couplings U in 1D. The corresponding phases in 2D and 3D will also be discussed and the collective modes calculated.

In the limit of many particles in a shallow confining harmonic potential, i.e. $N \rightarrow \infty$ and $V_2 \rightarrow 0$ but finite NV_2d^2 , the TF (or local density approximation) applies because the length scales over which the trapping potential and density varies are long compared to phase boundaries [21]. In TF the total chemical potential is given by the local chemical potential $\mu(\rho) = d\varepsilon/d\rho$, where ε and $\rho(r)$ are the local energy and density per site, and the trap potential as

$$\mu_{Tot} = \mu(\rho, U) + V_2 r^2 = \mu(0, U) + V_2 R^2. \quad (1)$$

It must be constant over the lattice and can therefore be set to its value at the edge or radius R of the atomic gas, which gives the last equation in (1). As we shall see later $\mu(\rho = 0, U) = -zt$ for both repulsive fermions and bosons, where $z = 2D$ is the number of neighbours in D dimensions.

We start with a 1D system of spin-balanced fermions with repulsive interactions. The energy per site can be calculated [22] from the Bethe ansatz. A good approximation for densities $\rho \leq 1$ and all $U \geq 0$ is

$$\mu(\rho, U) = -2t \cos(\pi\rho/\beta). \quad (2)$$

It is exact in both limits: $\beta(U \rightarrow \infty) = 1$ and $\beta(U \rightarrow 0) = 2$. For densities $1 < \rho \leq 2$ the chemical potential is: $\mu(\rho, U) = U - \mu(2 - \rho, U)$ [22]. The phase is a band insulator (BI) for $\rho = 2$, a MI for $\rho = 1$ and a Luttinger liquid (LL) [23] otherwise. The MI phase has a chemical potential gap $\Delta\mu = U + 4t \cos(\pi/\beta)$. It must match [22]

$$\Delta\mu(U) = U - 4t + 8t \int_0^\infty \frac{J_1(x)}{x[1 + \exp(xU/2t)]} dx, \quad (3)$$

where J_1 is the 1st Bessel function. Alternatively, one could as in [17] require that the energy: $\epsilon(1, U) = -2t(\beta/\pi) \sin(\pi/\beta)$, matches the exact result of the Bethe ansatz [22]. We prefer matching the chemical potentials because it insures that the Mott transitions are correct. The chemical potential is discontinuous at $\rho = 1$ by an amount $\Delta\mu = U - 4t + 8 \ln(2)t^2/U + \mathcal{O}(U^{-2})$, for $U \gg t$ whereas in the weakly repulsive limit the gap vanishes exponentially as $\Delta\mu = (8/\pi)\sqrt{Ut} \exp(-2\pi t/U)$. The density is now found by inserting (2) in (1). For $\rho \leq 1$ we obtain

$$\rho(r) = \frac{2\beta}{\pi} \arcsin(\sqrt{R^2 - r^2}/R_c), \quad (4)$$

where $R_c = 2\sqrt{t/V_2}$. The gap in the chemical potential Eq. (1) requires a density plateau at $\rho = 1$ [17–20]. We can now relate $\rho(0)$ to the radius R and the corresponding total number of atoms $N = (2/d) \int_0^R \rho(r) dr$ in the confined lattice for any U/t .

We are particularly interested in the critical radii R_n and the corresponding critical number of atoms $N_n =$

$(2/d) \int_0^{R_n} \rho(r) dr$, right when the MI and BI phases with $\rho(0) = n = 1, 2$ respectively appear in the center of the trap. For $U \gg t$ ($\beta \rightarrow 1$) the MI first appear in the center when $R_1 = R_c$ according to Eq. (4), and the corresponding number of particles is $N_1 = N_c$, where

$$N_c = \frac{4R_c}{\pi d} = \frac{8}{\pi d} \sqrt{\frac{t}{V_2}}. \quad (5)$$

Likewise, it follows that for $U \ll t$, where $\beta = 2$ and $\Delta\mu = 0$, the critical MI radius is shorter $R_1 = R_c/\sqrt{2}$ whereas the BI radius is $R_2 = R_c$. The corresponding critical number of atoms are $N_1 = (4R_c/\pi d) \int_0^1 \arccos(x^2) dx \simeq 0.847N_c$ and $N_2 = 2N_c$.

Returning to $U \gg t$ we must add the chemical potential gap $\Delta\mu = U - 4t$ to Eq. (1) when $\rho(r) > 1$. The critical radius, where then density just starts to exceed unity $\rho = 1_+$ in the core is: $R_1^+ = R_c \sqrt{U/4t}$, whereas the BI with $\rho = 2$ appears when $R_2 = R_c \sqrt{U/4t + 1}$. The corresponding number of atoms are

$$N_1^+ = \frac{2}{d} \sqrt{U/V_2} = N_c \frac{\pi}{4} \sqrt{U/t}, \quad (6)$$

and

$$N_2 = N_c \left[\frac{\pi}{4} \sqrt{U/t} + 1 \right]. \quad (7)$$

For general U we calculate $\Delta\mu(U)$ from Eq. (3) to find $\beta(U)$. Inserting (2) in (1) then gives the density, critical radii and the critical fillings as shown in Fig. 1. They interpolate smoothly between the analytical results $U \rightarrow 0$ and $U \gg t$ given above.

The numerical calculations in Refs. [25,18] find similar phase diagrams as the TF continuum limit $N \rightarrow \infty$ with a few important differences. The finite number of particles makes it impossible to resolve the exponentially small gap for $U \rightarrow 0$. The MI plateau in the density at $\rho = 1$ does not extend over a sufficient number of lattice sites, $R_1^+ - R_1 \lesssim d$, and the phase boundary cannot be resolved. Therefore, the critical point where the $\rho = 1$ MI state vanishes moves from $U_1 = 0$ in TF to $U_1 \simeq 0.8t$ in [18] and $U_1 \simeq 3t$ in [25]. As a consequence the phase diagrams of Refs. [25,18] acquire an additional phase transition at U_1 and $N \gtrsim N_1$ between phases with and without a “resolvable” $\rho = 1$ Mott transition. A similar phenomenon will occur at finite temperature, where the MI solid melts and the critical point moves to a finite U where $\Delta\mu(U) \simeq k_B T$.

The attractive Hubbard model ($U \leq 0$) tends to pair atoms in a Luther-Emery liquid (LE) [24]. The trap potential breaks translational invariance forming an atomic density wave (ADW) phase with oscillating density: $\rho(r_i) = \bar{\rho} + \delta\rho \cos(2\pi r_i/\lambda_{ADW})$ [24,17,19]. Here, $\bar{\rho}$ is the average density, $\delta\rho$ is the amplitude and $\lambda_{ADW} = 2d/\bar{\rho}$ the wavelength. The TF can be applied for the average density $\bar{\rho}$ as long as $R \gg \lambda_{ADW}$. As described in [17] the parametrization

$$\mu = U/2 - 2\alpha^2 t \cos(\pi\bar{\rho}/2), \quad (8)$$

is a good approximation for the EoS at all densities and $U \leq 0$. It satisfies the known properties for weak and strong attraction [22], when the prefactor is chosen as: $\alpha^2(U) = \pi \int_0^\infty J_0(x)J_1(x)/(1 + \exp(x|U|/2))(dx/x)$. It decreases from $\alpha(U = 0) = 1$ to $\alpha(U \rightarrow -\infty) = \sqrt{\pi \ln(2)t/|U|}$. No MI are formed in the LE at $\bar{\rho} = 1$ whereas a BI appears when $\rho = 2$ with radius $R_2 = 2\alpha t/V_2 = \alpha R_c$. The corresponding number of particles is

$$N_2 = 2\alpha N_c, \quad (9)$$

which is also shown in Fig. 1.

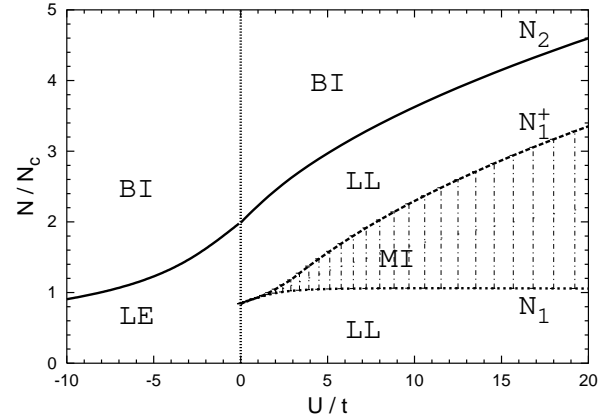


FIG. 1. Phase diagram of Fermions in a confined 1D optical lattice vs. U/t and number of atoms. The phases are denoted by the core state. For example, for $U > 0$ the BI phase has a band insulator core with $\rho = 2$ surrounded by a LL layer with $1 < \rho < 2$ again surrounded by a MI layer with $\rho = 1$ and finally a surface LL layer with $0 \leq \rho < 1$. The curves separate the phases where the MI appear (N_1), vanish (N_1^+) and a BI (N_2) appear in the center (see text). For $U \leq 0$ the LE liquid has a BI core when $N > N_2$.

Bosons do not experience Pauli blocking and therefore have a rather different phase diagram as fermions even for the same lattice, particle mass and interactions. Superfluid transitions to MI solid phases appear at integer filling, $n = 1, 2, 3, \dots$, above a critical coupling [25,26] $U_1 = 3.84t$, $U_2 = 6.2t$, and $U_n = 2.2nt$ for $n \gg 1$. Just above a critical coupling a Mott gap opens in the chemical potential compatible with a Kosterlitz-Thouless transition: $\Delta\mu_n \sim \exp(-const/\sqrt{U - U_n})$. When $U \gg U_n$ we have $\Delta\mu_n = U - 2zt$, whereas for $U \leq U_n$ there is no gap and $\Delta\mu_n = 0$. A good approximation to numerical results [25] for $U \gg t$ is the simple parametrization

$$\mu = nU + (U - \Delta\mu_n) \sin^2[(\rho - n)\pi/2] - zt. \quad (10)$$

Here, $n = \text{Int}[\rho]$ is the integer value of the density. The EoS has the correct chemical potential gaps $\Delta\mu_n$ built in for all U/t and the correct critical coupling U_n . The compressibility $d\rho/d\mu$ vanishes in the MI but diverges for densities approaching the MI as in [25]. For $U \gg t$

it has the same EoS as that for fermions, namely that of a non-interacting gas of a single fermion species. The strong on-site repulsion acts as Pauli-blocking similar to the case of strongly correlated nuclear liquid at high densities. The EoS can give the 1D Bose phase diagram at least qualitatively and generalizes the one shown in [27].

The critical radii for the MI transitions can be calculated in the same way as for fermions by inserting Eq. (10) in Eq. (1). We find

$$R_n^+ = \sqrt{nU/V_2}, \quad (11)$$

and

$$R_n = \sqrt{[nU - \Delta\mu_n]/V_2}. \quad (12)$$

The corresponding critical number of particles $N_n = (2/d) \int_0^{R_n} \rho(r) dr$ are shown in Fig. 2. When $U \gg t$ and $n \gg 1$

$$N_n^+ = N_{n+1} = \frac{4n}{3d} \sqrt{\frac{nU}{V_2}}. \quad (13)$$

Note, that $R_1 = R_c$ and $N_1 = N_c$ for $U \gg t$.

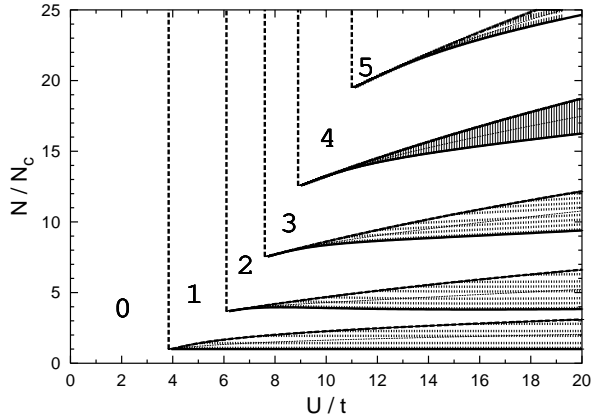


FIG. 2. Phase diagram for 1D bosons with EoS of Eq. (10). The parameter regions numbered $n = 0, 1, 2, 3, \dots$ form n MI phases of density $\rho = (0), 1, 2, \dots, n$ separated by $n + 1$ metal regions between core and surface. In the hatched areas the density has a MI core $\rho(0) = 1, 2, 3, \dots$, from below and up.

In higher dimensions $D = 2, 3$ the radii and critical fillings may be estimated from the scale of the energy and chemical potential. At densities up to unit filling the chemical potential varies on a scale $\sim t$ and therefore the size of the system remains of order $R_1 \sim \sqrt{2zt/V_2}$. Above unit filling the chemical potential gaps are of order $\sim U$ when $U \gg t$ and therefore the scale for the critical radii is unchanged: $R_{n+1} \simeq R_n^+ \simeq \sqrt{nU/V_2}$. The corresponding critical number of particles scales as $N_n = (2/d) \int_0^{R_n} \rho(r) d^D r \sim n^{1/D} (R_n/d)^D$. The phase diagram may, however, have additional phases. If high temperature superconductivity is described by the 2D Hubbard model [25,6], then we can expect that the MI

is replaced by an AFM phase around $\rho = 1$ surrounded by two dSC phases at densities lower (underdoped) and higher (overdoped). According to [28] phases with AFM and dSC order are mixed when $U \lesssim 8t$ but coexist when $U \gtrsim 8t$ with a first order transition between two densities. The dSC phases are again surrounded by two metal phases extending to the surface and the BI core respectively. It would therefore be most interesting to study the 2D phase diagram corresponding to the 1D case shown in Fig. 1 to find these phases, possible other phases such as spin glass, strange metal, striped, checker board, etc., and see how they vary with U/t and density. With extended interactions and hopping more MI phases at fractional filling [10] will appear which may separate into super-solid phases [8]. Mixing bosons and fermions leads to a number of new phases [11], and spin imbalance leads to novel pairing phases [29,30].

These and other phases can be observed by time-of-flight expansion, interference, noise correlations, molecule formation, etc. [1–4]. The collective modes has proven very useful observable in traps [31–33] and we will now calculate the modes for optical lattices. The equations of motion are in hydrodynamics and for a superfluid given by the equation of continuity and the Euler equation. Linearizing around equilibrium these lead to [21,33]

$$-m\omega^2 \mathbf{v} = \frac{1}{\rho} \nabla \left[\rho^2 \frac{d\mu}{d\rho} \nabla \cdot \mathbf{v} \right] + \nabla(\mathbf{f} \cdot \mathbf{v}) - \mathbf{f}(\nabla \cdot \mathbf{v}), \quad (14)$$

for the flow velocity \mathbf{v} . Here, the force from the harmonic trap potential is $\mathbf{f} = -\nabla(V_2 r^2) = -m\omega_0^2 \mathbf{r}$, introducing the trap frequency ω_0 as $V_2 = m\omega_0^2/2$.

The collective modes can be calculated analytically from Eq. (14) when the EoS is a simple polytrope: $\mu(\rho) - \mu(0) \propto \rho^\gamma$. At low densities the EoS optical lattices is on such a form for fermions with $\gamma = 2/D$. In 1D $\gamma = 2$ for both fermions and bosons according to Eq. (2) and (10). At higher densities the effective polytrope $\bar{\gamma} \equiv [\rho/(\mu - \mu(0))] d\mu/d\rho$ taken at central density $\rho(0) = \rho_c$ gave rather accurate collective modes in atomic traps [32,33]. For 1D fermions in an optical lattice

$$\bar{\gamma} = \frac{\pi\rho_c}{\beta} \cot(\pi\rho_c/2\beta), \quad (15)$$

for $\rho_c < 1$. In the non-interacting and attractive cases $U \leq 0$ with EoS given by Eq. (8), we also obtain Eq. (15) with $\beta = 1$. The same is the case for bosons with EoS of Eq. (10) whereas for $U \ll U_1$ the dilute bose EoS has $\bar{\gamma} = 1$ (see Fig. 3). We can expect a continuous change of $\bar{\gamma} = 1$ between these two limits. When $\rho_c \rightarrow 1$ and $U \gg t$ both bosons and fermions have $\bar{\gamma} \rightarrow 0$ whereas at $\rho_c = 1$ a MI forms in the center making the system incompressible (corresponding to $\bar{\gamma} \rightarrow \infty$).

As in 3D [33] the collective modes can be calculated in 1D generally for any polytropic EoS. Eq. (14) reduces to

$$\frac{1}{2}(1-x^2) \frac{d^2 v}{dx^2} - (\gamma+1)x \frac{dv}{dx} + \left(\frac{\omega^2}{\omega_0^2} - 1 \right) v = 0, \quad (16)$$

where $x = r/R$. The eigenfunctions are $v \propto F(-n, n + 2\gamma - 1, \gamma + 1, 2x - 1)$, where F is the hypergeometrical function. The corresponding 1D eigenvalues for multipoles with $n = 0, 1, 2, \dots$, nodes are

$$\frac{\omega^2}{\omega_0^2} = 1 + n[\gamma + 1 + (n - 1)/2]. \quad (17)$$

The dipole mode ($n = 0$) has constant flow velocity in all dimensions and by insertion in Eq. (14) has frequency $\omega/\omega_0 = 1$. It is independent of dimension, EoS (γ) and central density because the dipole mode corresponds to the whole cloud sloshing as a rigid body in the trap and thus only depends on the trap geometry in one direction (as long as $\rho_c < 1$). The breathing or monopole mode frequency has flow velocity $\mathbf{v} \propto \mathbf{r}$ and by insertion in Eq. (14) the monopole frequency is found to be $\omega^2/\omega_0^2 = 2 + \gamma D$, generally in D -dimensions.

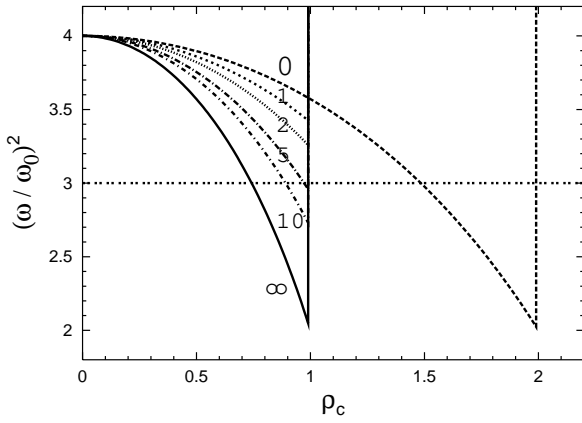


FIG. 3. 1D breathing mode frequency $\omega^2/\omega_0^2 = 2 + \bar{\gamma}$ vs. central density. Fermions are labelled with $U/t = 0, 1, 2, 5, 10, \infty$. Full curve is $U \gg U_1$ for both fermions and bosons. Dashed curve is for fermions with $U = 0$ and dotted curve is $\omega^2/\omega_0^2 = 3$ for bosons with $U \ll U_1$.

In Fig. 3 we show the 1D breathing mode frequency ($n = 1$) $\omega^2/\omega_0^2 = 2 + \bar{\gamma}$ with the effective polytrope $\bar{\gamma}$ given by Eq. (15). It decreases with increasing density until the MI appears in the core which is incompressible. Likewise we can expect that the collective modes will reveal the AFM state for the 2D Hubbard model. The dSC may only be expected to affect the EoS and collective modes weakly. Rotational vortices [29] or RF spectroscopy [34] may therefore be better signals of the dSC phases.

In summary, optical lattices provide a clean system where 1, 2 and 3D Hubbard and Bose-Hubbard models can be realized. The phase transitions between MI, LL, LE, superfluids and metals were calculated in 1D and scales estimated for 2+3D. Collective modes were calculated and found to be sensitive to the underlying EoS and phases. 2D optical lattices with fermions will therefore give direct insight in the high temperature superconductivity and the dSC+AFM phases vs. interaction strength, doping and temperature.

-
- [1] M. Greiner *et al.*, Nature **419**, 51 (2002).
 - [2] T. Stöferle *et al.*, Phys. Rev. Lett. **92**, 130403 (2004). H. Moritz, T. Stöferle, K. Günther, M. Köhl, T. Esslinger, *ibid.* **94**, 210401 (2005); *ibid.* **96**, 030401 (2006).
 - [3] F. Gerbier *et al.*, Phys. Rev. A **72**, 053606 (2005) and Phys. Rev. Lett. **96**, 090401 (2006).
 - [4] G. Thalhammer *et al.*, cond-mat/0510755.
 - [5] D.J. Scalapino, Physics Reports **250**, 329 (1995). P.W. Anderson, Science **235**, 1196 (1987).
 - [6] W. Hofstetter *et al.*, Phys. Rev. Lett. **89**, 220407 (2002)
 - [7] L.-M. Duan, Phys. Rev. Lett. **95**, 243202 (2005). A. Isacsson and S. M. Girvin, cond-mat/0506622
 - [8] V.W. Scarola and S. Das Sarma, Phys. Rev. Lett. **95**, 033003 (2005)
 - [9] A.S. Sørensen, E. Demler, M.D. Lukin, cond-mat/0405079.
 - [10] H. Heiselberg, Phys. Rev. A **73**, 013628 (2006).
 - [11] D.-W. Wang, M.D. Lukin, E. Demler, Phys. Rev. A **72**, (R)051604 (2005)
 - [12] J. Hubbard, Phys. Rev. B **17**, 494 (1978).
 - [13] M.P.A. Fisher, P.B. Weichman, G. Grinstein, D.S. Fisher, Phys. Rev. B **40**, 546 (1989).
 - [14] D. Jaksch *et al.*, Phys. Rev. Lett. **81**, 3108 (1998).
 - [15] W. Zwerger, J. Opt. B **5**, 9 (2003).
 - [16] B. Paredes, P. Fedichev, J.I. Cirac, P. Zoller, Phys. Rev. Lett. **87**, 010402 (2001).
 - [17] V.L. Campo & K. Capelle, Phys. Rev. A **72**, 061602 (2005)
 - [18] X.-J. Liu, P.D. Drummond, H. Hu, Phys. Rev. Lett. **94**, 136406 (2005).
 - [19] G. Xianlong *et al.*, cond-mat/0506570; cond-mat/0512184; cond-mat/0603118.
 - [20] M. Rigol, A. Muramatsu, Phys. Rev. A **69**, 053612 (2004) and Opt. Commun. **243**, 33 (2004). Rigol *et al.*, Phys. Rev. Lett. **91**, 130403 (2003).
 - [21] C.J. Pethick and H. Smith, *Bose-Einstein Condensation in Dilute Gases*, Cambridge Univ. Press, 2002.
 - [22] E.H. Lieb and F.Y. Wu, Phys. Rev. Lett. **20**, 1445 (1968).
 - [23] J.M. Luttinger, J. Math. Phys. N.Y. **4**, 1154 (1963).
 - [24] A. Luther and V.J. Emery, Phys. Rev. Lett. **33**, 589 (1974).
 - [25] G.G. Batrouni, R.T. Scalettar and G.T. Zimanyi, Phys. Rev. Lett. **65**, 1765 (1990). P. Niyaz, R.T. Scalettar, C.Y. Fong, and G.G. Batrouni, Phys. Rev. B **44**, 7143 (1991)
 - [26] T.D. Kühner and H. Monien, Phys. Rev. B **58**, R14741 (1998). N. Elstner and H. Monien, cond-mat/9905367
 - [27] C. Kollath, U. Schollwöck, J. von Delft, and W. Zwerger, Phys. Rev. A **69**, R031601 (2004)
 - [28] M. Capone and G. Kotliar, cond-mat/0603227.
 - [29] M.W. Zwierlein *et al.*, Science **311**, 492 (2006); Nature **435**, 1047 (2005).
 - [30] G.B. Partridge *et al.*, Science, 23 December 2005 (10.1126/science.1122876) (cond-mat/0511752).
 - [31] J. Kinast *et al.*, Phys. Rev. Lett. **92**, 150402 (2004). M. Bartenstein *et al.*, Phys. Rev. Lett. **92**, 203201 (2004)
 - [32] H. Hu, A. Minguzzi, X.-J. Liu, M.P. Tosi, Phys. Rev. Lett. **93**, 190403 (2004).
 - [33] H. Heiselberg, Phys. Rev. Lett. **93**, 040402 (2004).
 - [34] C. Chin *et al.*, Science **305** 1128 (2004).